Al-Qadisiyah JournalFor Engineering Sciences 18 (2025) 001–010

Contents lists available at: http://qu.edu.iq

Al-Qadisiyah Journal for Engineering Sciences

Journal homepage: https://qjes.qu.edu.iq

Research Paper

Bond characteristics of steel bars in lightweight concrete incorporating various steel fibres

Shirin Rady and Adnan Al-Sibahy

Civil Engineering Department, College of Engineering, The University of Al-Qadisiyah, Iraq.

ARTICLE INFO

Article history:
Received 04 January 2024
Received in revised 10 March 2024
Accepted 11 February 2025

keyword:
Lightweight concrete
Steel fibres
Bond strength
Anchorage length
Lapped length

ABSTRACT

Reinforcement-concrete bond is a topic that has been extensively investigated with reference to normal concrete. Scanty attention, however, has been devoted so far to lightweight aggregate concrete, which is the subject of this study. The bond behaviour of steel bars embedded in lightweight concrete containing expanded clay and steel fibres is investigated for different types of fibrous reinforcement. Sixteen beam-like specimens were reinforced with deformed steel bars of two diameters (12 or25 *mm*) and contained three types of steel fibres with an aspect ratio equal to 60 (straight microfibres, hooked fibres, or hybrid fibres). Preliminarily, the physical and mechanical properties of the mixes (either plain or fibre-reinforced) were investigated, and comparisons were made with the provisions of Model Code 10. The addition of fibres increases concrete density (up to 8%), concrete compressive strength (up to 28%) and tensile strength in bending (up to 163%, "splitting strength"), especially in the case of hybrid fibres. The tests on bond in the beam-like specimens show that bond strength is markedly affected by both the bar diameter and the bonded length, as the larger the bar diameter, the lower the bond strength. Suitable amendments are suggested for some expressions proposed in MC 10.

1. Introduction

Lightweight concrete has shown large utilized in the construction field especially for the precast applications [1–4]. The advantages of lightweight concrete were understood over 50 years ago in countries such and US, UK, Sweden, and Italy [5]. It considers one of the structural choices for improving the low ratio of strength to weight as the self-weight of such kind of concrete is about two-third of the normal weight concrete. Besides its role in upgrading the strength to weight ratio, lightweight concrete also has several advantages in terms of improving thermal insulation, fire resistance, and acoustic isolation. Previous studies have clarified that the thermal conductivity of the lightweight concrete is about half that of normal concrete due to its low density and porous structure that traps air-being a poor heat conductor. Such a lower value of conductivity means that heat will not pass through the material easily, employing lower interior heating and/or cooling requirements of buildings. This is one of sustainability parameters where in situations of rising energy costs and increasing concerns about climate change, the former reduction is most welcome [6–9]. The idea of adding fibres to the concrete matrices was proposed as it improves the majority of the concrete characteristics. This includes maximum tensile strength and the induced strain, compressive strain at ultimate load, potential of energy absorption and toughness, fatigue strength, shear resistance, crack distribution. Such technique can be used for both plain and reinforced concrete. When the fibres are combined with steel reinforcements, the brittleness characteristic is minimized, concrete deformability is increased, and there is less congestion of secondary reinforcements needed in crucial areas of structures intended for seismic zones. Consequently, longer service life has been noted for the fibre-reinforced concrete than conventional concrete due to the function of fibres in inhibiting the growth of cracks inside the concrete [1, 8, 10–13]. In the design of reinforced concrete structures, the characteristics of bond between the interior concrete surfaces and reinforcing bars are the critical consideration as they assumed to be integrated into one specimen. Previous studies [14, 15] have demonstrated that the pressure parallel to the direction of steel bars induces the crucial tension between concrete and rebar reinforced. To evaluate the former behaviour, beam test method is usually experimentally adopted. Several experimental measurements [16–18] illustrated that the bond-slip aspect is significantly affected by the variation in the concrete composition. Consequently, the determined lap and anchorage lengths which are the design criteria for the reinforced concrete members are changed accordingly. Due to the differences in the composition between the normal and lightweight concretes, understanding the bond-slip behaviour of structural lightweight concrete needs for further investigation. Despite a lot of research works have been recently published, however, limited investigations have been conducted on the bond strength behaviour of lightweight concrete containing steel fibres in different geometries. In this study, micro, hook end, and hybrid steel fibres were used to evaluate the bond strength of lightweight concrete in terms of bond stress-bar slip curve using beam specimens. A comparison was also made with some formulas suggested by relevant codes of practice.

*Corresponding Author.
E-mail address: adnan.alsibahy@qu.edu.iq ; Tel: (+964 782 355-4721) (A. Al-Sibahy)

https://doi.org/10.30772/qjes.000.000.000

Nomenclature:

List of variables:

A_{st}	The cross-sectional area of a single leg of confining steel bar (mm^2)
C_{max}	The maximum distance value of C_x and C_y
C_{min}	The minimum distance value of C_x and C_y
f_{bd}	The design bond strength
F_{bdo}	The basic bond strength
f_{cm}	The compressive strength of cylinder specimen (MPa)
k_m	The adequacy of the transverse reinforcement confinement
S_t	The spacing of the longitudinal reinforcement (mm)

Greek Symbols:

η_1	The legs of the confinement transverse reinforcements
η_2	The case of bond between the steel bar and concrete
η_b	The number of anchored or lapped bars subjected to tension forces
σ_{sd}	The initiated stresses in the anchored reinforcement
ϕ	The anchored steel bar diameter (mm)

2. Experimental work

An extended wide experimental programme was set out to measure the bond-slip behaviour of expanded clay concrete containing different geometries of steel fibres using beam specimens. The preliminary mechanical properties of the concrete mixes were also measured. The next sections describe the details of the experimental work performed in this study.

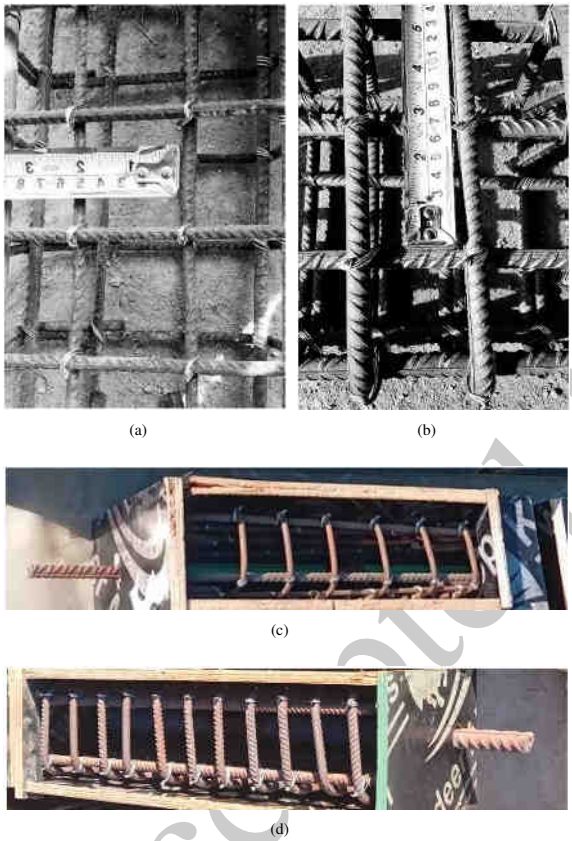

Figure 1. Ribs of reinforcing rebars; (a) $\phi 6$ *mm* and $\phi 8$ *mm*, (b) $\phi 10$ *mm*, (c) $\phi 12$ *mm*, and (d) $\phi 25$ *mm*.

2.1 Materials

According to the study's goals, expanded clay lightweight aggregate was used as a coarse aggregate to create lightweight concrete mixes with a maximum particle size of 8 mm and an absorption ratio of 8–12% after 24 hours. For all lightweight concrete mixtures, ordinary Portland cement that complied with EN BS 197-1 [19] was used as a binder. The ingredient of fine aggregate was in form of natural sand, and it was consistence with the limitations of EN BS 882.1992 [20] and have a maximum particle size and sulfate content of 4.75 mm and 0.173%, respectively. To achieve a suitable consistency ($100 \pm 10 mmslump$), Caplast Super-R superplasticizer (SP) admixture was used during the mixing processes. It has a specific gravity of 1.2 at 25. The beam-like specimens were reinforced with longitudinal bars (two diameters) and stirrups (three diameters) as indicated in Table 1. Figure 1 shows ribs of the reinforcing rebars. Steel fibres (either microfibres or hooked fibres, aspect ratio = 60) were adopted, as shown in Fig. 2. The length, diameter of micro and hooked steel fibres were 13.01 mm, 0.22 mm and 30.48mm, 0.51mm, respectively. In addition, combination of the former steel fibres was also investigated to identify the effect of hybridization technique on the produced lightweight concrete mixes.

2.2 Selection of the concrete mix

A suitable lightweight concrete mix was designed to have a strength value of more than 35 MPa at 28 days age based on the procedure suggested by [21] and the recommendation of previous studies [22]. Following numerous trial mixes with varying W/C ratios to reach the specified slump value (100 ± 10 *mm*), the reference lightweight concrete mix's mix proportions are 425.6 kg/m^3 cement: 447.58 kg/m^3 sand: 259.72 kg/m^3 expanded clay and $W/C = 0.38$. Thereafter, steel fibres were added to the selected lightweight concrete mix with a total ratio of 1.5% by volume. This implies producing a further three lightweight concrete mixes. To ensure keeping the same consistency for the lightweight concrete mixes containing steel fibres, admixture of superplasticizer (SP) was used with a dosage of 1% from the cement weight implying reduction to the original W/C to be 0.35. Taking into consideration using two diameters of deformed steel bars in formulation the beam specimens intended to be tested for the bond strength aspect, this gives eight different beam specimens, as shown in Table 2.

Table 1. The steel bars' geometrical and mechanical characteristics.

Role of the reinforcement	Bar dia. (*mm*)	Ultimate stress F_u (MPa)	Yield stress F_y (MPa)
Pull out reinforcement (longitudinal bars)	25	678.23	418.36
	12	680.30	419.96
Transverse reinforcement	10	663.65	420.00
	08	661.71	420.55
	06	658.47	421.21

Table 2. The lightweight concrete mixtures utilized in this study.

No.	Symbol	Micro steel fibre %	Hook end steel fibre (%)	SP (%)	Diameter of the steel bar (*mm*)
1	l-R-12	0.00	0.00	0.00	12.00
2	l-R-25	0.00	0.00	0.00	25.00
3	l-M-12	1.50	0.00	1.00	12.00
4	l-M-25	1.50	0.00	1.00	25.00
5	l-H-12	0.00	1.50	1.00	12.00
6	l-H-25	0.00	1.50	1.00	25.00
7	l-HY-12	0.75	0.75	1.00	12.00
8	l-HY-25	0.75	0.75	1.00	25.00

2.3 Preparation of the test moulds

Based on the method suggested by [23, 24], wooden moulds were designed to perform tests on bond strength. Two configurations of wooden moulds were selected. The first mould configuration was designed with dimensions of 1260 mm × 150 mm × 240 mm (l×w×h) to suit the requirements of beam specimens incorporating embedded steel bar of $\phi 25$ *mm*. The second mould configuration was designed with dimensions of 800 mm × 100 mm × 180 mm (l×w×h) to suit the requirements of beam specimens incorporating embedded steel bar of $\phi 12$ *mm*. All wooden moulds were produced in the form of two parts split at the mid-span with gabs of 60 mm and 50 mm for the first and second configurations, respectively, as illustrated in Figs. 3 and 4. The details of the wooden moulds with their steel reinforcements ready for casting are shown in Fig. 5.

(a) (b)

Figure 2. Steel fibres; (a) micro steel fibre, (b) hook end steel fibre.

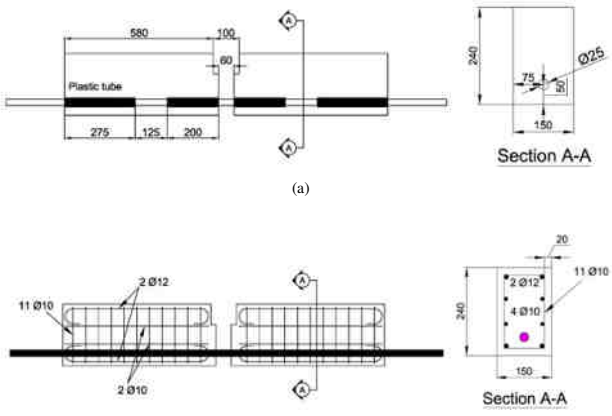

Figure 3. Beam specimens reinforced with steel bar of $\phi 25$ *mm*; (a) dimensions of the moulds; (b) reinforcement details.

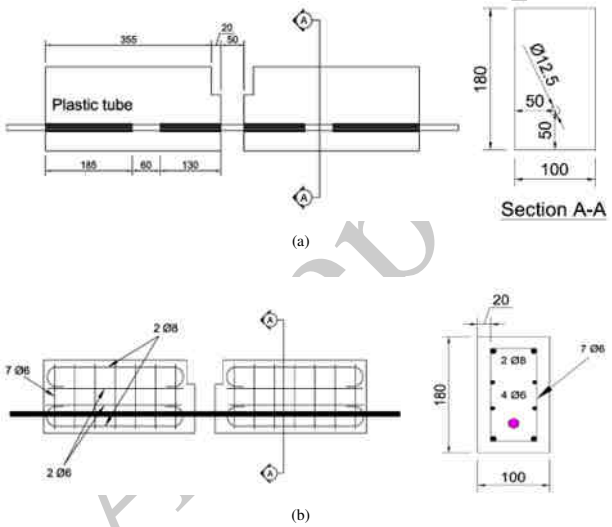

Figure 4. Beam specimens reinforced with steel bar of $\phi 12$ *mm*; (a) dimensions of the moulds; (b) reinforcement details.

2.4 Mixing, casting, and curing operations

In this study, the BS EN12390-2 [25] instructions for the mixing operations were followed. After that, the casting of the freshly mixed concrete was made in form of three layers; and the Poker vibrator was used for compacting each layer. When the compaction process has been finished, the beam specimens were covered with a nylon sheet to maintain moisture for the cement hydration. After 24 hours, the beam specimens were demolded and kept at the laboratory temperature with in controlled hygro-thermal conditions. Sixteen beam specimens of reinforced lightweight concrete were cast, half of them were fabricated with steel bar of 12mm in diameter and the other were fabricated with steel bar of 25mm in diameter. On this basis, the prepared beam specimens were divided in to four groups: the first represents the control beam specimens (without steel fibres); the second represents those formulated with micro steel fibres; the third represents those fabricated with hooked end steel fibres, and the fourth represents those incorporated hybrid steel fibres (50% micro and 50% hooked end). The average value of two specimens was taken into consideration for each testing case. Figure 6 shows the casting operations for the beam specimens. Cube and cylinder specimens with dimensions of $150 \times 150 \times 150mm$ and $100 \times 200mm$, respectively, were also cast to measure the compressive and splitting tensile strengths as well as density feature.

Figure 5. The wooden molds with the steel reinforcements.

Figure 6. The wooden molds with the steel reinforcements.

2.5 The measured parameters

Firstly, the preliminary mechanical properties of the investigated lightweight concrete mixes were measured at 7 and 28-days age. This was done through running the compressive and tensile strengths as well as density tests. The previous tests were conducted in accordance with BS EN 12390-3 [26], BS EN 12390-6 [27] and BS EN12390-7 [28], respectively. The bond strength test was then conducted to assess the bond-slip feature for the beam specimens. The latter test was running out in accordance with the recommendations of RILEM RC6 Parts 1 and 2, respectively [29] using a stiff steel rig with capacity of 1000 kN. The arm of the internal forces was defined based on the recommendations of RILEM (1973)-RC6 [29] in addition to the procedure described in [30] which have identical procedure to the recommendations of EN 10080:2005 [31].On this basis, two T-steel sections with a thickness of 15 *mm* were adhered to the interior concrete surfaces at the upper middle aperture of the beam using ProBuild epoxy, as shown in Fig. 7a-c. Accordingly, the resulted arms for the beam samples reinforced with $\phi 25$ *mm* and $\phi 12$ *mm* were 150mm and 100mm, respectively. The loading rate was 2 KN /Sec, and the applied load was manually controlled. Besides, the corresponding flexural load-deflection features of the reinforced beam specimens were recorded using dial-gauge and LVDT at the lower corner of the concrete part (Point 2) and the middle of steel bar (Point 3), as shown in Fig. 8. The latter was connected to data logger. The test continued until the occurrence of failure and the load-crack history was reported. For each tested case, the failure modes and critical zones were also

monitored. In order to check the accuracy obtained results, a nondestructive test method using Digital Image Correlation (DIC) was followed. For this, all beam specimens were painted in a white color and the critical failure zones were dotted so that a correlation between the applied load and the corresponding deformations can be obtained based on the duration of the test.

(a)

(b) (c)

Figure 7. Define the arm of the internal forces; (a) Two (T) steel sections with a thickness of 15 *mm* used as a stiff steel hinge; (b) and (c) ProBuild epoxy used to adhere the steel hinge to the beam specimen.

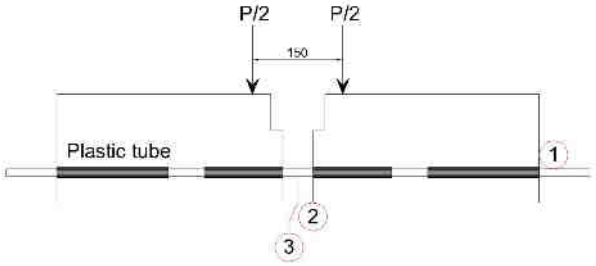

Figure 8. Locations of the deformation measurements.

3. Results and discussion

3.1 Preliminary mechanical properties

The results of the preliminary mechanical properties are shown in Figs. 9, 10, and 11. It is obvious that all density values of the tested specimens (determined after drying for 28 days) are below the maximum specified limit for the structural lightweight concrete (i.e., no more than 1800 kg/m^3), as shown in Figure 9. However, inclusion of steel fibres increases the density of lightweight-concrete specimens by up to 130 kg/m^3. This is clearly known, as the mass per unit volume of the steel fibre is higher than that of cement and the inclusion of steel fibres was carried out based on the volume substitution. In addition, the difference in the density between types of fibre may be related to geometry and interaction with the concrete surfaces as they have different on the interfacial transition zone. For the compressive strength, the reference lightweight concrete mix recorded 37.30 MPa at 28-day age, as shown in Fig. 10. The percentage increase in the strength from the age of 7 days to 28 days was 25.5%. The corresponding percentage increases for the L-M, L-H and L-HY mixes were 9.5%, 15.2% and 21%, respectively.

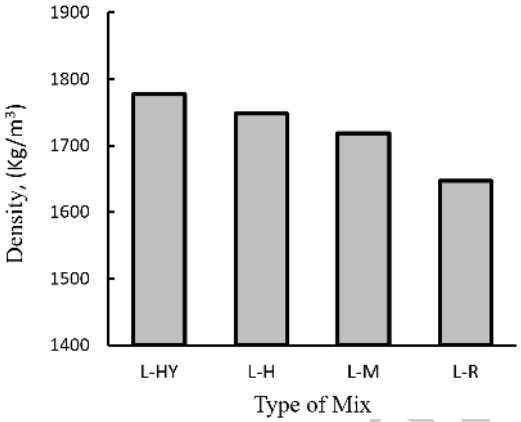

Figure 9. Density values of the investigated lightweight concrete mixes.

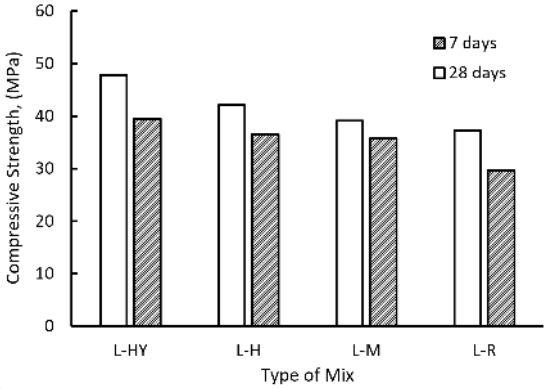

Figure 10. Compressive strength values of the investigated lightweight concrete mixes.

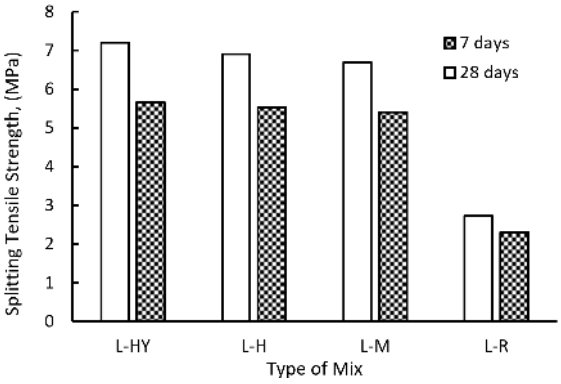

Figure 11. Splitting tensile strength values of the investigated lightweight concrete mixes.

This indicative for the effect of the steel fibre on the inner structure of concrete in which inconsistency interfacial transition zone can be obtained due to voids released around the steel fibre. Nevertheless, the overall strength level increased as the added fibres resisting higher applied loads with tendency to achieve ductile material. Previous studies [1, 12] have also found similar behaviour. Among the four tested lightweight concrete mixes, mix L-HY revealed the highest compressive strength of 47.8 MPa at 28-day age. Such an attitude explains the advantage of the hybridization technique where both adhesion and ductility characteristics can be obtained. The percentage increase in the compressive strength for the former mix at 28-day age compared to the reference one is 28A similar tendency to that of compressive strength was also noted for the splitting tensile strength feature where the L-HY mix showed the highest value at 7.2 MPa, as shown in Fig. 11. In contrast to what was noted in the compressive

strength, the growth of tensile strength from 7 to 28-day age was higher for the concrete mixes containing steel fibres. The percentage increase in the value of splitting tensile strength at 28-day age compared to those at 7 days were 18.6%, 24%, 24.7% and 27.2% for the L-R, L-M, L-H and L-HY mixes, respectively. This can be attributed to the nature of the applied tensile load and the role of the steel fibres in eliminating the tensile carks which normally leads to failure of concrete specimens by means of tailoring the propagated cracks.

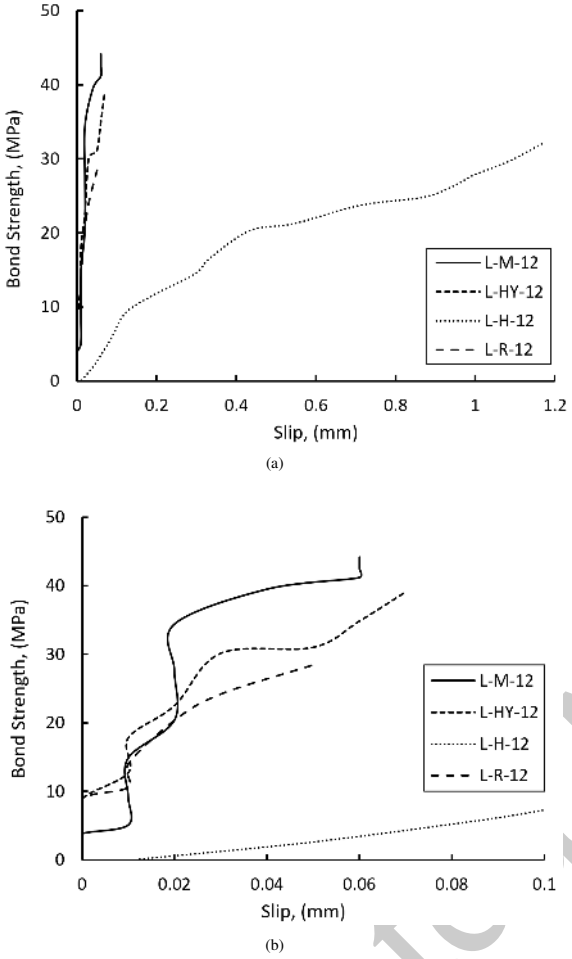

Figure 12**.** Bond-slip values for the beam specimens reinforced with steel bar of ϕ12 *mm*; (a) the whole beam specimens, (b) enlarge of critical zone.

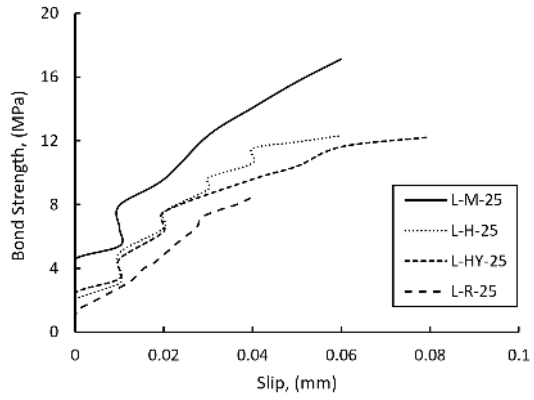

Figure 13**.** Bond -slip values for the beam specimens reinforced with steel bar of ϕ25 *mm*.

3.2 Bond strength behaviour

The bond strength results in the form of the shear-slip relationship for the beam specimens reinforced with steel bars of 12 *mm* and 25 *mm*, respectively, are shown in Figs. 12 and 13. The average value of two specimens was taken into consideration for each testing case, as the variation between the readings obtained of individual samples for two identical elements did not exceed 10%. Obvious improvements have been observed in the recorded pullout strength for the fibrous lightweight concrete beams compared to those of normal lightweight concrete. The highest values were noted for the specimens with mirco-steel fibres and the percentage increases in the pullout strength were 55% and 104% for the beam specimens reinforced with steel bars of ϕ12 *mm* and ϕ25 *mm*, respectively. This was followed by beam specimens containing hybrid and hook end steel fibres. Such behaviour can be explained by the role of the steel fibres which interact with the surrounding concrete and surfaces of the steel bar result in an increase in friction resistance. Similar results were also noted by Campione et. al [1]. In terms of the slip, the fibrous lightweight concrete beams exhibited more slip value than those of normal lightweight concrete. In both cases of embedded steel bars (i.e., ϕ12 *mm* and ϕ25 *mm*), the slip value of reference specimens was in the range of 0.05 mm. On the other hand, the beam specimens having micro and hybrid steel fibres showed slip values of 0.06 and 0.07mm, respectively. It is interesting to observe that the beam specimen containing hook end steel fibres and reinforced with steel bar ofϕ12 *mm* showed a slip value twenty times higher than of other tested specimens, as shown in Fig. 12a and b. It could be due to invisible experimental error or related to the delay in the occurrence of the whole failure as the fibres in combination with traditional steel reinforcements reduce the brittleness of concrete combined with the hook end nature of the added steel fibre. Consequently, higher ductility is obtained. Except for the L-H-12, all beam specimens exhibited some slip beyond 20 kN of the applied load. For higher loads, the slip and the load increased simultaneously, as shown in Fig. 12 and Fig. 13. For the comparison purposes, converting the measured data of load-slip to bond strength feature by dividing the load value on the embedded area of steel bar reveals that the smallest bar diameter produces the highest bond strength. This is scientifically accepted as the increasing of the steel bar diameter means more contact surface area is available with the concrete, hence increasing the possibility of existing weakness points along the interaction zone. The latter reduces the obtained bond strength. For this, approximately three times bond strengths were noted for the beam specimens reinforced with steel bars of ϕ12 *mm* compared with those of ϕ25 *mm*. Similar behaviour was also noted by P. Bamonte et al. [32].

3.3 Load-deflection behaviour

The results obtained for the load-deflection feature at the lower end corner of the concrete beam (Point 2) and underneath of the reinforced steel bar (Point 3) are shown in Fig. 14 up to Fig. 17. Identical behaviour to that noted for the bond-slip was also observed where the highest bending loads were recorded for the fibrous lightweight concrete beams containing micro steel fibres at 104 kN and 172 kN for the beam specimens reinforced with steel bars of ϕ12 *mm* and ϕ25 *mm*, respectively. Furthermore, the specimens containing hybrid and hook end steel fibres demonstrated the highest deflection value due to the bending load for the beam specimens reinforced with ϕ12 *mm* at 16 mm, as shown in Fig. 14. Whilst lower deflection value for Point 2 was recorded for the beam specimens reinforced with ϕ25 *mm* at 8 mm which is corresponding to the beam specimen containing micro steel fibre, as shown in Fig. 15. This is indicative for more stiffness of the latter beam specimen where a clear restrain for the tendency of the concrete specimen to have more bowing was noted. However, comparing to the case of reference lightweight concrete, the former attitude of the beam specimens reinforced with ϕ25 *mm* characterized as a ductile material as double value of deflection has been acquired. Figures 16 and Fig. 17 illustrate the load- vertical deflection of Point 3 located in the mid-span section of the reinforcing bar. Similar behaviour to that of Point 2 was also observed. However, larger magnitude of vertical deflection was noted for the beam specimens reinforced with steel bar of ϕ12 *mm* reaching to 40 *mm*, as shown in Fig. 16. Except for the L-H-12, these specimens also showed steeper load-deflection curve up to 80% of the ultimate load, thereafter rapid deflection was shown. The same cannot be said for beam specimens reinforced with steel bar of ϕ25 *mm*, as the maximum deflection reach only 7 mm for L-M-25, as shown in Fig. 17. This could be due to the geometric characteristic of the deformed steel bars and the differences in their stiffness. It is worth mentioning that these results are compatible with the results obtained for Point 2. The reason for that may be related to the unique load that was used in performing the test, in addition to the near distance between the instruments used for measuring the vertical deformations at the end corner of concrete and the steel bar.

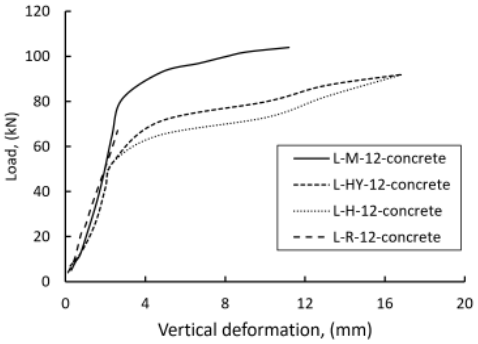

Figure 14**.** Load-deflection values at the lower end corner (Point 2, Fig. 6) for the beam specimens having steel bar of 12 *mm*.

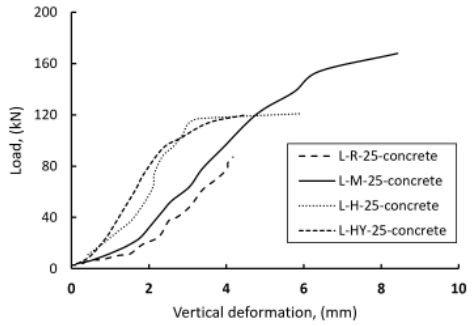

Figure 15**.** Load-deflection values at the lower end corner (Point 2, Fig. 6) for the beam specimens having steel bar of 25 *mm*.

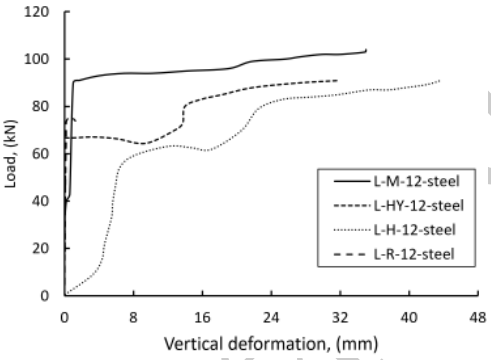

Figure 16**.** Load-deflection values measured in the mid-span section of the reinforcing bar (Point 3, Fig. 6) for the beam specimens having steel bar of 12 *mm*.

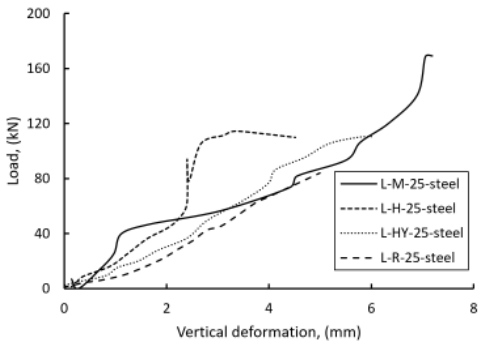

Figure 17**.** Load-deflection values measured in the mid-span section of the reinforcing bar (Point 3, Fig. 6) for the beam specimens having steel bar of 25 *mm*.

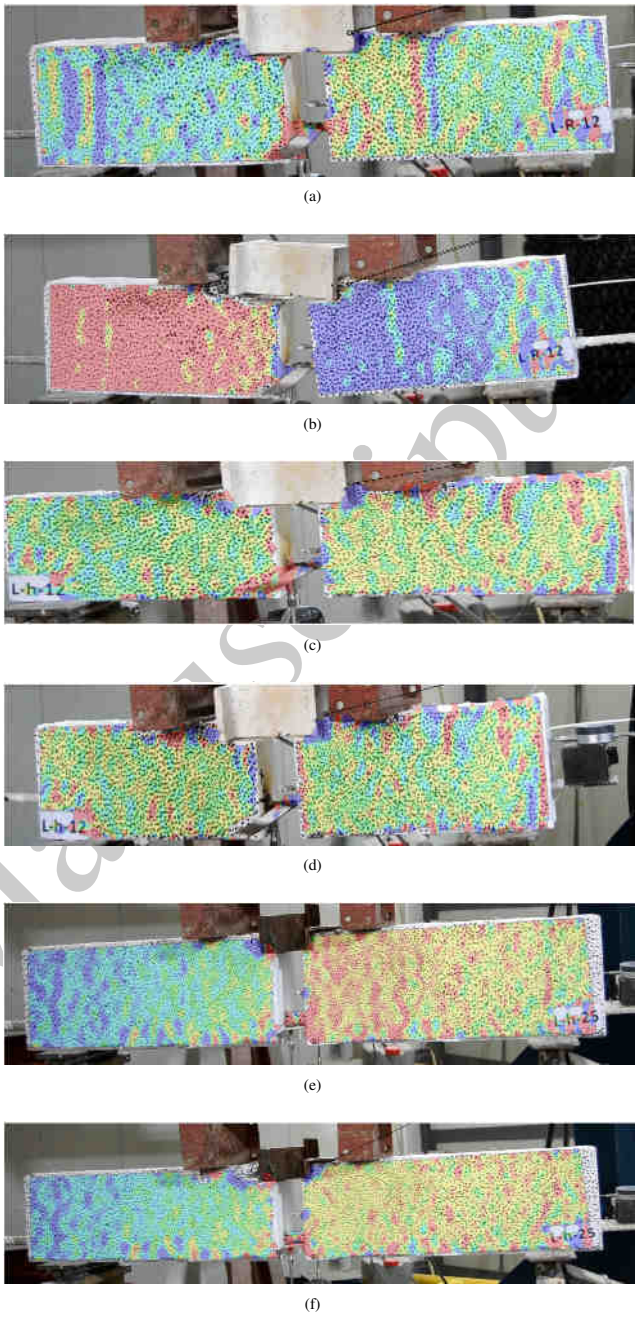

Figure 18**.** Failure modes monitored via Digital Image Correlation: (a,b) Specimen L-R-12 (no fibres), load levels LL = 50% and 100% of the failure load, respectively; (c,d) Specimen L-H-12 (microfibres), LL = 50% and 100%; and (e,f) Specimen L-H-25 (hooked fibres), LL = 50% and 100%.

To verify the deflection measurements, DIC mechanism was adopted as mentioned in section 2.5. The results obtained using the aid of GOM correlate have been presented in Table 3. The highest and lowest percentage differences compared with the measured deflection values using dial gauge technique for the lower corner of concrete (Point 2) were -35.5% and +2%, respectively. The corresponding percentage differences for Point 3 were +36.4% and -14%, respectively. Such close agreement is evidence that the experimental tests were performed with good quality control. Figures 18a to f show the contour lines for three selected beam specimens (L-R-12, L-H-12, and L-H-25) at 50% and 100% of the failure load using Epsilon (Y) rate.

3.4 Failure modes and crack history

In general, all lightweight concrete beam specimens exhibited similar failure modes. As the load increases, the separated steel plate at the upper part of the beam specimen transfers to a steel hinge. The latter causes transverse

compression stress on the opposite interior faces the concrete parts. Consequently, pullout stresses for the embedded steel bar will take place, as shown in Fig. 19a. Following this, cracks start to initiate around the embedded bar and the interface of concrete, subsequently extended to the exterior surfaces till the ultimate slip value is obtained, as shown in Fig. 19b. On the other hand, flexural failure mode was noted for both concrete and the free region of steel bar, as shown in Fig. 20a. This was in terms of crushing the concrete regions underneath the point of load application. The latter is subsequent with pullout cracks, as shown in Fig. 20b.

(a) (b)

Figure 19**.** Pull out failure modes of the beam specimens: (a) debonding, (b) pullout cracks.

(a) (b)

Figure 20**.** Flexural failure modes: (a) flexural rupture, (b) concrete crushing at the edges associated with rebar slipping.

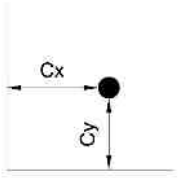

Figure 21**.** Illustrates the chosen values of Cx and Cy based on the spacing between the steel bars and concrete cover.

Table 4 illustrates the values of the first crack load and their locations. The highest first crack load was observed for the beam specimen comprising micro steel fibres reinforced with steel bar of $\phi 25$ *m*m at 119.1 kN. However, this load acquires the lowest ratio to the ultimate load at 0.71. Following this description, beam specimens containing hook end steel fibres showed the highest ratio at 0.98 meaning more time is needed to propagate the first crack. This may be due to the function of the end geometry of this type of fibre in preventing the creation of cracks by tailoring mechanism. The locations of the first crack were underneath the point of applied load, around the embedded bar and combined between them for the reference, micro and hook end and hybrid specimens, respectively.

3.5 Comparison with the code of practice

For the purpose of exploring the structural applications of the experimental measurements, the findings of this study have been compared with the CEB-FIP [33] code. The latter indicated that the bond strength can be determined as shear stress of the embedded steel bar in a concrete using the following Equation.

$$\tau_{bu,split} = 6.5\eta_2 \left(\frac{f_{cm}}{25}\right)^{0.25} \left(\frac{25}{\phi}\right)^{0.25} \left[\left(\frac{C_{min}}{\phi}\right)^{0.33} \left(\frac{C_{max}}{\phi}\right)^{0.1} + K_m K_{tr}\right] \quad (1)$$

where η_2 is a parameter reflecting the case of bond between the steel bar and concrete with recommended values of 1.0 and 0.7 for the good and other bond cases, respectively, f_{cm} represents the compressive strength of cylinder specimen (Mpa), ϕ is the anchored steel bar diameter (mm), C_{min} is the minimum distance value of C_x and C_y, while C_{max} is the maximum distance value of C_x and C_y as per in Fig. 21,k_m is a parameter representing the adequacy of the transverse reinforcement confinement taken as 12 when the steel bars are confined inside a bend of links in an angle not less than 90°and k_{tr} is a parameter accounted based on Eq 2.

$$K_{tr} = \eta_1 A_{st}/(\eta_b \phi S_t) \leq 0.05 \quad (2)$$

where η_1 refers to the legs of the confinement transverse reinforcements, A_{st} represents the cross-sectional area of a single leg of confining steel bar (mm^2), η_b reflects to the number of anchored or lapped bars in the surfaces subjected to tension forces, while S_t represents the spacing of the longitudinal reinforcement using for additional confinement (mm). Following Eq. 1 and considering the value η_2 of all lightweight concrete beam specimens as 1.0, the theoretical and measured bond strength values are presented in Table 6. Note that Eq. 1 seems to underestimate the bond-strength in the beam specimens reinforced with the smaller-diameter bar (diameter = 12 mm). The highest difference between the theoretically calculated and measured values of the bond strength was observed for the lightweight concrete beam containing micro steel fibres. This can be attributed to the effect of such a kind of steel fibre which enhances the bond feature between the concrete and lower diameter of reinforcement. Consequently, Eq. 1 needs amendment in order to fit with the experimental results of this study. Table 6 presents the proposed values of (η_2) based on the outcome of this study.

In RC structural design of reinforced concrete, Eqs. 3, 7, and 8 are introduced by CEB-FIP [33] to evaluate the lengths of anchored and spliced bars (L_b and L_p), respectively.

$$L_b = \frac{\phi \sigma_{sd}}{4 f_{bd}} \geq L_{b.min} \quad (3)$$

where ϕ refers to diameter of the embedded bar in (mm), σ_{sd} represents initiated stresses in the anchored reinforcement resulting from the bond determined using Eq. 4, while $f_{bd}$is the design bond strength as per in Eq.5 which is calculated on the base on the basic bond strength (f_{bd0}). The former term is described in Eq. 6.

$$\sigma_{sd} = \alpha_1 f_{yd} - (F_h/A_b) \quad (4)$$

$$f_{bd} = 2 f_{bd0} - 0.4 P_{tr} \quad (5)$$

$$f_{bd0} = \eta_1 \eta_2 \eta_3 \eta_4 \left(\frac{f_{ck}}{25}\right)^{0} .5/\gamma_{cb} \quad (6)$$

where $\alpha_1$refers to the $A_{s.cal}/A_{s.ef}$ ratio in which the $A_{s.cal}$ represents the area of reinforcement calculated to be adequate for the design criteria, while $A_{s.ef}$ is the provided area of reinforcement. f_{yd} represents the ratio of f_y/γ_{cb} in which γ_{cb} is a coefficient equivalent to the bond safety factor (normally used as 1.5). F_h refers to the developed force on the anchored bar and for the case of straight. tension bar it is taken as zero, A_b represents the cross sectional area of the anchored rebar, P_{tr} refers to the average compression stress in a direction perpendicular to the surface with the prospect to splitting failure (MPa), η_1 is a coefficient referring to the condition of the embedded rebar and it is recommended to be 1.75 for bar in normal condition,η_2 is a coefficient suggested to be 1.0 for the condition of normal and good bond, otherwise it was suggested to be 0.7, η_3 is a coefficient corresponding to the bar diameter and it equal to 1.0 for $\phi \leq 25$ *mm* and $\left(\frac{25}{\phi}\right)^{0}$.3 for bars with $\phi > 25$ *mm*, η_4 represents the strength of embedded steel bar and its values are 1.2, 1, 0.85, 0.75, 0.68 when the values of f_{yk} are 400, 500, 600, 700, 800 MPa, respectively, whereas f_{ck} is corresponding to the value of compressive strength of concrete (Mpa).

$$L_p = 0.7 \frac{yd}{4 f_{bd}} \geq L_{p.min} \rightarrow In\ tension \quad (7)$$

$$L_p = \frac{\partial}{4 f_{bd}} \left(f_{yd} - F_h/A_s\right) \geq L_{p.min} \rightarrow In\ compression \quad (8)$$

$CEB-FIP$ [33] indicated that the minimum values of L_b and L_p taken as below:

Table 3. Comparison between the vertical displacements at points 2 and 3 measured by means of dial gauges and calculated via Digital Image Correlation.

No.	Symbol	Ultimate load, (kN)	Ultimate vertical displacement at point 2 (mm)		Differences	Ultimate vertical displacement at point 3 (mm)		Differences
			Dial gauge reading	DIC reading		Dial gauge reading	DIC reading	
1	L-R-12	067.0	03.2	04.3	-25.6	03.6	05.8	-37.9
2	L-R-25	084.0	05.0	04.9	+02.0	05.0	05.9	-15.3
3	L-M-12	104.0	11.0	09.7	+13.4	12.0	17.0	-29.4
4	L-M-25	172.0	08.5	09.6	-11.5	08.0	09.3	-14.0
5	L-H-12	082.0	17.0	21.0	-19.0	45.0	33.0	+36.4
6	L-H-25	120.0	06.0	09.3	-35.5	05.5	08.3	-33.7
7	L-HY-12	092.0	16.5	14.0	+17.9	32.0	-	-
8	L-HY-25	120.0	05.0	07.3	-31.5	06.5	08.0	-18.8

Table 4. First-crack loads of the lightweight-concrete beam specimens.

No.	Symbol	First crack load (kN)	Ratio of first crack load/ ultimate load	Location of the first crack
1	L-R-12	48.0	0.72	Underneath the point of applied load
2	L-R-25	60.0	0.70	Underneath the point of applied load
3	L-M-12	92.1	0.89	Around the embedded bar
4	L-M-25	119.1	0.71	Around the embedded bar
5	L-H-12	73.8	0.98	Around the embedded bar
6	L-H-25	113.1	0.93	Around the embedded bar
7	L-HY-12	71.5	0.78	Around the embedded bar underneath of the applied load
8	L-HY-25	114.5	0.95	Around the embedded bar underneath of the applied load

Table 5. First-crack loads of the lightweight-concrete beam specimens.

No.	Symbol	Experimentally measured values of, (τ) (average value) (Map)		Theoretical values of (τ) calculated from Eq. 1 (Mpa)	
		$\phi 12$ *mm*	$\phi 25$ *mm*	$\phi 12$ *mm*	$\phi 25$ *mm*
1	L-R	28.45	08.95	19.76	14.38
2	L-M	44.16	17.12	19.99	14.55
3	L-H	32.04	12.33	20.36	14.82
4	L-HY	39.06	12.22	21.02	15.30

Table 6. The proposed values of η_2 to be used in calculation the bond strength

No.	Symbol	Values of η_2	
		$\phi 12$ *mm*	$\phi 25$ *mm*
1	L-R	1.43	0.62
2	L-M	2.20	1.17
3	L-H	1.57	0.83
4	L-HY	1.85	0.79

Table 7. Values of anchorage and lap lengths of the embedded steel bar.

Beam class	Beam Symbol	Value of L_b length in (mm)			Value of L_p length in (mm)		
		Eq. 3	Eq. 3 including the data of Table 6	Differences%	Eq. 8	Eq. 8 including the data of Table 6	Differences%
Beam specimens reinforced with steel bar of $\phi 12$ *mm*	L-R-12	275	173	-37	290	183	-37
	L-M-12	319	106	-67	347	116	-67
	L-H-12	245	137	-44	278	155	-44
	L-HY-12	228	101	-56	280	124	-56
Beam specimens reinforced with steel bar of $\phi 25$ *mm*	L-R-25	598	1071	+79	495	887	+79
	L-M-25	676	549	-19	565	459	-19
	L-H-25	577	729	+26	490	619	+26
	L-HY-25	525	703	+34	457	613	+34

$$L_{b,min} > max\ \{0.3\ \phi\ f_{yd}\ /\ (4 f_{bd}); 10\phi; 100\ mm\}$$
$$L_{b,min} > max\{0.7\phi f_{yd}/(4 f_{bd}); 15\phi; 200\ mm\}$$

If the reinforcements are assumed to be under the action of compression as in the case of this study, Table 7 presents the calculated anchorage and lap (L_b and L_p) lengths based on Eq. 3 and Eq. 8, respectively. Inclusion the proposed η_2 values shown in Table 6 in determining the value of basic bond strength (f_{bd0}), the former $L_b$and L_p values should be corrected as in Table 7. It can be seen that all beam specimens reinforced with steel bar of $\phi 12$ *mm* xhibited lower calculated values for L_b and L_p compared with their corresponding measured values reaching to (-56%). This can be explained by the superior effect of the added steel fibres at such boundary conditions. The absent of steel fibres reduces the amount of pullout strength required to achieve the failure especially for the larger reinforce diameter (i.e., $\phi 25$ *mm*) as per in in the

specimen L-R-25. Thus, additional embedded length of steel bar is required to withstand such tendency. Nevertheless, inclusion of steel fibres minimizes the former reduction of pullout strength as per in the beam specimens of L-M-25, L-H-25 and L-HY-25. This commentary on the calculated values of L_b and L_p is worth to be noticed and taken into consideration to do an appropriate revision suit the cases of normal and fibrous lightweight concrete specimens.

4. Conclusions

Reinforcement-concrete bond in light-weight concrete, either plain or fibre-reinforced with straight, hooked or hybrid fibres, is investigated in this experimental study, where the concrete grade 37 MPa for the plain concrete face to the rather small density 1600 (kg/m^3). The main findings of this study are:

- As already observed in previous studies found in the literature, the addition of steel fibres to lightweight mixes improves the mechanical properties of the concrete; hybrid fibres (equally subdivided between straight and hooked fibres, total fibre content 1.5% by mass of the concrete) are the most efficient, as they increase substantially the compressive and the tensile strength (up to 28% and 163%, respectively, in the tests performed in this study).
- The addition of steel fibres, however, increases the density of the concrete (by up to 8% in the lightweight concretes tested in this study, 1850 kg/m^3) and brings lightweight concretes close to the conventional lower bound for ordinary concretes (2000 kg/m^3, no fibres); fibres, however, increase concrete toughness. • The pull-out resistance of large-diameter bars (25 *mm* in this study) is smaller than that of small diameter bars (12 *mm* in this study) in terms of ultimate bond strength, both in plain and in fibre reinforced concretes; a possible explanation is that in large-diameter anchored bars there is a greater probability for the bar-concrete interface to be affected by concrete defects due to the heterogeneous natura of the material.
- The design equations proposed by MC 10 to evaluate the ultimate capacity and the length of an anchored or spliced bar seem to be markedly on the safe side, and amendments are proposed to include the beneficial effect that steel fibres have on bond behaviour.

Authors' contribution

All authors contributed equally to the preparation of this article.

Declaration of competing interest

The authors declare no conflicts of interest.

Funding source

This study didn't receive any specific funds.

Data availability

The data that support the findings of this study are available from the corresponding author upon reasonable request.

Acknowledgements

The authors would like to express deep thanks for the technical assistance of the laboratory staff at the College of Engineering-University of Al-Qadisiyah.

REFERENCES

[1] G. Campione, C. Cucchiara, L. La Mendola, and M. Papia, "Steel–concrete bond in lightweight fiber reinforced concrete under monotonic and cyclic actions," *Engineering Structures*, vol. 27, no. 6, pp. 881–890, 2005. [Online]. Available: https://doi.org/10.1016/j.engstruct.2005.01.010

[2] G. Campione, S. Mindness, and G. Zingone, "Compressive stress-strain behavior of normal and high-strength carbon fiber concrete reinforced with steel spirals," *Materials Journal*, pp. 27–34, Jan. 1999. [Online]. Available: https://doi.org/10.14359/424

[3] P. Balaguru and A. Foden, "Properties of fiber reinforced structural lightweight concrete," *Engineering, Materials Science*, vol. 93, no. 1, pp. 62–78, 1996. [Online]. Available: https://doi.org/10.14359/9833

[4] M. Papia, "Mechanical properties of steel fibre reinforced lightweight concrete with pumice stone or expanded clay aggregates," *Materials and Structures*, vol. 34, no. 1, pp. 201–210, 2001. [Online]. Available: https://doi.org/10.1007/BF02480589

[5] R. Karthika, V. Vidyapriya, K. Nandhini Sri, K. Merlin Grace Beaula, R. Harini, and M. Sriram, "Experimental study on lightweight concrete using pumice aggregate," *Materials Today: Proceedings*, vol. 43, pp. 1606–1613, 2021, international Conference on Advanced Materials Behavior and Characterization (ICAMBC 2020). [Online]. Available: https://doi.org/10.1016/j.matpr.2020.09.762

[6] K. Y. Juankum, "Cracking mode and shear strength of lightweight concrete beams," Ph.D. dissertation, National University fo Singapore, 2011. [Online]. Available: https://core.ac.uk/download/48649291.pdf

[7] N. Lee, J. Pae, S.-H. Kang, H. ki Kim, and J. Moon, "Development of high strength lightweight cementitious composites using hollow glass microsphere in a low water-to-cement matrix," *Cement and Concrete Composites*, vol. 130, p. 104541, 2022. [Online]. Available: https://doi.org/10.1016/j.cemconcomp.2022.104541

[8] C.-G. Go, J.-R. Tang, J.-H. Chi, C.-T. Chen, and Y.-L. Huang, "Fire-resistance property of reinforced lightweight aggregate concrete wall," *Construction and Building Materials*, vol. 30, pp. 725–733, 2012. [Online]. Available: https://doi.org/10.1016/j.conbuildmat.2011.12.081

[9] H. M. S. Aslam, A. U. Rehman, K. C. Onyelowe, S. Noshin, M. Yasin, M. A. Khan, A. Latif, H. M. U. Aslam, and S. Hussain, "Evaluating the mechanical and durability properties of sustainable lightweight concrete incorporating the various proportions of waste pumice aggregate," *Results in Engineering*, vol. 24, p. 103496, 2024. [Online]. Available: https://doi.org/10.1016/j.rineng.2024.103496

[10] M. Hassanpour, P. Shafigh, and H. B. Mahmud, "Lightweight aggregate concrete fibre reinforcement - A review," *Constr. Build. Mater.*, vol. 37, p. 452–461, 2012. [Online]. Available: https://10.1016/j.conbuildmat.2012.07.071

[11] E. Güneyisi, M. Gesoğlu, and S. İpek, "Effect of steel fiber addition and aspect ratio on bond strength of cold-bonded fly ash lightweight aggregate concretes," *Construction and Building Materials*, vol. 47, pp. 358–365, 2013. [Online]. Available: https://doi.org/10.1016/j.conbuildmat.2013.05.059

[12] A. Al-Sibahy and S. Mashshay, "Development of hybrid ecc columns subjected to concentric and eccentric loading," *Structures*, vol. 28, pp. 309–320, 2020. [Online]. Available: https://doi.org/10.1016/j.istruc.2020.08.080

[13] N. A. Libre, M. Shekarchi, M. Mahoutian, and P. Soroushian, "Mechanical properties of hybrid fiber reinforced lightweight aggregate concrete made with natural pumice," *Construction and Building Materials*, vol. 25, no. 5, pp. 2458–2464, 2011. [Online]. Available: https://doi.org/10.1016/j.conbuildmat.2010.11.058

[14] S. Gali and K. V. Subramaniam, "Cohesive stress transfer and shear capacity enhancements in hybrid steel and macro-polypropylene fiber reinforced concrete," *Theoretical and Applied Fracture Mechanics*, vol. 103, p. 102250, 2019. [Online]. Available: https://doi.org/10.1016/j.tafmec.2019.102250

[15] X. Gao, N. Li, and X. Ren, "Analytic solution for the bond stress-slip relationship between rebar and concrete," *Construction and Building Materials*, vol. 197, pp. 385–397, 2019. [Online]. Available: https://doi.org/10.1016/j.conbuildmat.2018.11.206

[16] X. Liu, Y. Liu, T. Wu, and H. Wei, "Bond-slip properties between lightweight aggregate concrete and rebar," *Construction and Building Materials*, vol. 255, p. 119355, 2020. [Online]. Available: https://doi.org/10.1016/j.conbuildmat.2020.119355

[17] M. Ahmadi, A. Kheyroddin, A. Dalvand, and M. Kioumarsi, "New empirical approach for determining nominal shear capacity of steel fiber reinforced concrete beams," *Construction and Building Materials*, vol. 234, p. 117293, 2020. [Online]. Available: https://doi.org/10.1016/j.conbuildmat.2019.117293

[18] T. Uygunoğlu, W. Brostow, O. Gencel, and B. Topçu, "Bond strength of polymer lightweight aggregate concrete," *Polymer Composites*, vol. 34, no. 12, pp. 2125–2132, 2013. [Online]. Available: https://doi.org/10.1002/pc.22621

[19] I. P. Sfikas, A. Kanellopoulos, K. G. Trezos, and M. F. Petrou, "Durability of similar self-compacting concrete batches produced in two different eu laboratories," *Construction and Building Materials*, vol. 40, pp. 207–216, 2013, special Section on Recycling Wastes for Use as Construction Materials. [Online]. Available: https://doi.org/10.1016/j.conbuildmat.2012.09.100

[20] S. Gali and K. V. L. Subramaniam, "Specification for aggregate from natural sources for concrete," 1992.

[21] A. Al-Sibahy and R. Edwards, "Mechanical and thermal properties of novel lightweight concrete mixtures containing recycled glass and metakaolin," *Construction and Building Materials*, vol. 31, pp. 157–167, 2012. [Online]. Available: https://doi.org/10.1016/j.conbuildmat.2011.12.095

[22] C. S. and B. L., *Lightweight aggregate concrete Science, Technology, and Applications*. William Andrew, 2000. [Online]. Available: https://www.semanticscholar.org/paper/Lightweight-aggregate-concrete

[23] M. Valcuende and C. Parra, "Bond behaviour of reinforcement in self-compacting concretes," *Construction and Building Materials*, vol. 23, no. 1, pp. 162–170, 2009. [Online]. Available: https://doi.org/10.1016/j.conbuildmat.2008.01.007

[24] A. Al-Sibahy and M. Sabhan, "Corrosion effects on the bond behaviour of steel bars in self-compacting concrete," *Construction and Building Materials*, vol. 250, p. 118568, 2020. [Online]. Available: https://doi.org/10.1016/j.conbuildmat.2020.118568

[25] A. C31/C31M-24b, "Standard practice for making and curing concrete test specimens in the field," *ASTM*, 2009. [Online]. Available: https://doi.org/10.1520/C0031_C0031M-24B

[26] "Testing hardened concrete, part 3: Splitting tensile strength of test specimens," 2009. [Online]. Available: https://doi.org//science/article/abs/pii/S0167844218306438

[27] "Testing hardened concrete, part 6: Splitting tensile strength of test specimens," 2009.

[28] "Testing hardened concrete, part 7: Density of hardened concrete," 2009. [Online]. Available: https://doi.org//science/article/abs/pii/S0167844218306438

[29] Rilem, *RILEM Technical Recommendations for the testing and use of construction materials*. H Australia, 1994. [Online]. Available: https://doi.org/10.1201/9781482271362

[30] P. Desnerck, G. D. Schutter, and L. Taerwe, "Bond behaviour of reinforcing bars in self-compacting concrete: experimental determination by using beam tests," *Mater Struct*, vol. 43, p. 53–62, 20110. [Online]. Available: http://dx.doi.org/10.1617/s11527-010-9596-6

[31] B. Standards, "Bond strength and surface geometry," 2005.

[32] P. F. Bamonte and P. G. Gambarova, "High-bond bars in nsc and hpc: Study on size effect and on the local bond stress-slip law," *Journal of Structural Engineering*, vol. 133, no. 2, pp. 225–234, 2007. [Online]. Available: https://doi.org/10.1061/(ASCE)0733-9445(2007)133:2(225)

[33] CEB-FIP, "Model code 2010 - first complete draft, volume 1," *fib CEB-FIP*, 2010. [Online]. Available: https://doi.org/10.35789/fib.BULL.0055

How to cite this article:
Shirin Rady and Adnan Al-Sibahy, (2025). 'Bond characteristics of steel bars in lightweight concrete incorporating various steel fibres', Al-Qadisiyah Journal for Engineering Sciences, 18(XX), pp. 001-010. https://doi.org/10.30772/qjes.2025.154566.1417